
Counterfactual Analysis in Dynamic Models: Copulas and Bounds

Martin B. Haugh

Imperial College

m.haugh@imperial.ac.uk

Raghav Singal

Dartmouth College

singal@dartmouth.edu

Abstract

We provide an explicit model of the causal mechanism in a structural causal model (SCM) with the goal of estimating counterfactual quantities of interest (CQIs). We propose some standard dependence structures, i.e. *copulas*, as base cases for the causal mechanism. While these base cases can be used to construct more interesting copulas, there are uncountably many copulas in general and so we formulate optimization problems for bounding the CQIs. As our ultimate goal is counterfactual reasoning in dynamic models which may have latent-states, we show by way of example that filtering / smoothing / sampling methods for these models can be integrated with our modeling of the causal mechanism. Specifically, we consider the “cheating-at-the-casino” application of a hidden Markov model and use linear programming (LP) to construct lower and upper bounds on the casino’s winnings due to cheating. These bounds are considerably tighter when we constrain the copulas in the LPs to be time-independent. We can characterize the entire space of SCMs obeying *counterfactual stability (CS)*, and we use it to negatively answer the open question of Oberst and Sontag [18] regarding the uniqueness of the Gumbel-max mechanism for modeling CS. Our work has applications in epidemiology and legal reasoning, and more generally in counterfactual off-policy evaluation, a topic of increasing interest in the reinforcement learning community.

History. This version: May 26, 2022

1 Introduction

It’s been discovered that a casino has been cheating at one of its games over a period of several weeks. Instead of using a fair die, it has been found to adopt a (hidden) Markov policy whereby it occasionally swaps out the fair die for a loaded die. The earnings of the casino in this game over the time period in question are known and a court is now asking how much of these earnings were due to cheating? Or consider someone who has recently died from cancer. The exact progression of her disease is unknown. What is known, however, is that over a period of time prior to her diagnosis, her insurance company adopted a strategy of denying her regular scans for this type of cancer even though these scans should have been covered by her policy. Had these scans gone ahead, the cancer may have been found early and the patient’s life saved. Now a court wants to know the probability that her life would have been saved had the routine scans been permitted?

Answering these questions requires a counterfactual analysis as they require us to imagine a world where a certain policy and outcome took place *given* that a different policy and outcome were actually observed. Such questions belong on the third rung of Pearl’s so-called ladder of causation [20] and require a *causal mechanism* to answer them. Our goal in this paper is to provide a simple framework for answering these kinds of questions in dynamic latent-state Markov models. In particular, we can summarize our contributions as follows:

- (i) We propose a structural causal model (SCM) which explicitly recognizes that modeling the full range of counterfactual possibilities at each node in the SCM requires specifying a joint probability distribution over counterfactual random variables at that node.
- (ii) Specifying the aforementioned probability distribution amounts to specifying the dependence structure or *copula* of the counterfactual random variables. We therefore introduce the language of copulas to this kind of analysis and describe some well known copulas as benchmarks.
- (iii) Because uncountably many copulas can be consistent with observational data, in general we can only hope to provide bounds on the counterfactual quantities of interest (CQI's), e.g. casino earnings due to cheating, or the probability the patient would have survived had scans been permitted. We therefore formulate optimization problems to construct lower and upper bounds on the CQI's. Because our problems are dynamic in nature, we impose an easily justifiable *time consistency* requirement on the copulas and this results in considerably tighter bounds.
- (iv) Our modeling approach can easily handle constraints on the causal mechanism. For example, we show that the recently proposed counterfactual stability (CS) property [18] can be modeled (at least in our application) via linear constraints in our optimization problems. We also resolve some open questions of [18] regarding (a) the sensitivity of the CQI to the choice of SCM and (b) whether other approaches (beyond the use of the Gumbel-max “trick” they propose) can be found to generate counterfactuals while satisfying the CS property.
- (v) We show by way of example that filtering / smoothing / sampling methods for dynamic latent-state models can be integrated with our modeling of the causal mechanism. Specifically, we consider the “cheating-at-the-casino” hidden Markov model (HMM) application and use linear programming (LP) to construct lower and upper bounds on the casino's winnings due to cheating. To the best of our knowledge, we are the first to provide bounds on a CQI in a dynamic latent-state model.

One potential weakness of our approach is that we assume the model structure is known. This assumption is necessary to perform the filtering and smoothing steps that calculate the distribution of the latent-states conditional on the observations. Without this step we cannot compute bounds on the CQI's. This is not a major limitation, however, as there are many interesting and successful applications, e.g. [3, 4], where the model structure (though perhaps not the model parameters) is assumed to be known. (If the model parameters are not known they can easily be estimated given sufficient data.) Moreover, if our focus is not on bounds but rather on the investigation of interesting causal mechanisms then our framework would still be useful for counterfactual off-policy evaluation irrespective of whether or not latent variables are present.

There are two streams of work that are closely related to our work. The first relates to work by researchers including Pearl and colleagues, e.g. [2, 22, 11, 6, 19, 16], on constructing bounds on CQI's. These papers focus on static models and generally consider binary variables. They also use LP techniques to construct bounds and as these problems are much smaller they have been able to develop analytic expressions for these bounds. The tightness of these bounds then depends on whether observational and / or experimental data are available and whether structural assumptions such as monotonicity are imposed. With the exception of [16], these papers do not assume the structure of the graph is known. In contrast, we do assume the graph structure is known but only so as to perform the filtering and smoothing steps for computing the hidden-state distribution conditional on the observations. We also explicitly discuss the dependence structure, i.e. copulas, and identify some interesting copulas as base cases for our analysis.

A second stream of related research [5, 13, 18, 23] is more recent and concerns counterfactual off-policy evaluation for dynamic models, usually in a reinforcement learning context. These papers recognize the need to model the causal mechanism but they generally fix a single causal mechanism [5] or invoke a possibly desirable property such as CS [18, 23] and then implicitly fix the causal mechanism via the Gumbel-max trick. [13] also aims to extend the Gumbel-max approach but their choice of causal mechanism is one that minimizes the variance when estimating CQI's. In summary, none of these approaches explicitly account for all of the possible causal mechanisms, i.e. joint distributions or copulas, and therefore they don't consider the construction of lower and upper bounds on the CQI's.

2 Preliminaries: Structural Causal Models

We first review structural causal models (SCMs) in the context of directed acyclic graphs (DAGs), e.g. [19]. Each node in the DAG represents a random variable. The random variables are divided into two types: *endogenous* variables V_i which are modeled explicitly, and *exogenous* variables which are not modeled explicitly and represent background noise. Each endogenous variable V_i has a (potentially empty) set of endogenous parent variables pa_i , an exogenous parent variable U_i , and an associated function f_i which uniquely determines V_i as a function of pa_i and U_i , i.e. $V_i = f_i(pa_i, U_i)$. Throughout the paper we will make the following assumption.

Assumption 1. *The exogenous variables are independent.*

Assumption 1 is consistent with the assumption of no unobserved confounding in our SCMs. This is important for dynamic latent state models where we need to know the structure of the graph for filtering, smoothing and sampling. Figure 1a displays a simple example of an SCM. This SCM is intended to model the outcome V_O of a surgical procedure on a patient. This outcome depends on the hospital V_H where it is performed, the surgeon V_S who performs it and an exogenous variable U_O representing some background noise. The endogenous variables are therefore V_O , V_H and V_S . There are also exogenous variables U_H and U_S which essentially model the random mechanism determining the hospital where the procedure is performed and the surgeon who performs it. None of the exogenous variables have parents and because of Assumption 1, each exogenous variable has a single outbound arrow to the single endogenous variable with which it is associated. (This also implies that V_H and V_S are independent so that the possible surgeons work across all possible hospitals and knowing the hospital where the procedure is performed tells us nothing regarding the identity of the surgeon who performs it.) Finally, the joint distribution of the endogenous variables is completely determined by the marginal distribution of the exogenous variables.

We remark it is quite common and wlog when dealing with association and intervention questions, i.e. questions from the first two rungs, to take the exogenous variables to be $U(0, 1)$ random variables. This follows because we can use the inverse-transform method from Monte-Carlo simulation (e.g. [9]) to generate each V_i with the correct probability distribution conditional on pa_i . We refer to [19] for further details on SCMs.

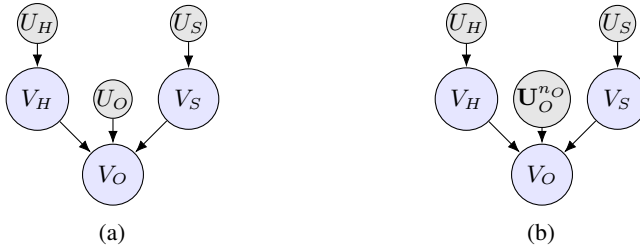


Figure 1: (a) A simple SCM modeling the outcome V_O of a surgical procedure on a patient. The outcome depends on the hospital V_H where it is performed, the surgeon V_S who performs it and an exogenous variable U_O . (b) An SCM for the same problem but now explicitly recognizing (via boldface font) that $U_O^{n_O}$ is a vector of n_O $U(0, 1)$ random variables.

2.1 Counterfactual Reasoning

Suppose there are three possible hospitals, two possible surgeons and two possible outcomes (“Good”, “Bad”) for the surgical procedure. We observe the first surgeon performed the procedure in the first hospital and that the outcome was “Bad”. A natural question to ask is why this outcome occurred? Was it because of the hospital or surgeon or some combination of the two? Or perhaps it was just “bad luck”? More specifically, we might be interested in answering the *counterfactual* question:

“Would the outcome have been “Good” if the procedure was performed by surgeon # 2 in hospital # 3 given that it was actually performed by surgeon # 1 in hospital # 1 and the outcome was “Bad”?

It’s well known how to answer a question like this in an SCM and there are three steps required:

1. **Abduction.** Use the evidence (hospital # 1, surgeon # 1 and outcome “Bad”) to infer the conditional distribution of U_O .

2. **Action.** Modify the SCM by removing the arrows from U_H to V_H and from U_S to V_S and replace them with the appropriate functions $V_H = 3$ and $V_S = 2$.
3. **Prediction.** Use the modified model and inferred distribution of U_O to predict V_O .

These steps are widely understood - e.g. see [19] - but in our opinion there seems to be some confusion over modeling the exogenous variables to reflect the full range of possible causal mechanisms. This is perhaps not too surprising as most causal questions focus on the first two rungs (“Association” and “Intervention”) of Pearl’s “ladder of causation”. While modeling the distribution of the exogenous variables is clearly important for answering association and intervention questions, we need to go further than this when answering counterfactual questions which are represented by the third rung on Pearl’s ladder. In particular, we need to model the full causal mechanism and we will speak of exogenous random *vectors* rather than exogenous random variables.

2.2 The Causal Mechanism

Let n_i denote the number of possible *settings* of pa_i with the understanding that if V_i has no parents then $n_i = 1$. Referring to our surgical procedure example in Figure 1a for example, V_O has 2 endogenous parents, V_H and V_S , which have 3 and 2 possible values, respectively. Therefore pa_O has $n_O = 3 \times 2 = 6$ possible settings. In general, each possible setting of pa_i requires its own separate $U(0, 1)$ random variable. This is most easily seen by recognizing that $V_O \mid (\text{pa}_O = s)$ defines a *distinct* random variable for each $s = 1, \dots, n_O$. Since $n_O = 6$ in our example, there are six distinct random variables that must be modeled. Moreover, these six random variables might be independent, or they might display positive or negative dependence. One way to handle this is to associate each $V_O \mid (\text{pa}_O = s)$ with a distinct $U(0, 1)$ random variable. The *dependence structure* among these uniforms is then what determines the dependence structure among the elements of $\{V_i \mid (\text{pa}_i = s)\}_{s=1}^{n_i}$. Returning to our general SCM notation, we can therefore write

$$\begin{aligned} V_i &= f_i(\text{pa}_i, \mathbf{U}_i^{n_i}) \\ &= \sum_{s=1}^{n_i} f_{i,s}(U_{i,s}) \mathbf{1}_{\{\text{pa}_i=s\}} \end{aligned} \quad (1)$$

for an arbitrary endogenous node V_i where $\mathbf{U}_i^{n_i} := [U_{i,1} \dots U_{i,n_i}]$ is an $n_i \times 1$ vector of $U(0, 1)$ random variables, $\text{pa}_i = s$ represents (via a slight abuse of notation) the event that pa_i take on their s^{th} possible setting, and $\mathbf{1}_{\{\cdot\}}$ denotes the indicator function. The representation (1) allows us to model $\{V_i \mid (\text{pa}_i = s)\}_{s=1}^{n_i}$ and capture any dependence structure among these n_i random variables by specifying the joint multivariate distribution of $\mathbf{U}_i^{n_i}$. Since the univariate marginals of $\mathbf{U}_i^{n_i}$ are known (they are all $U(0, 1)$), specifying the multivariate distribution of $\mathbf{U}_i^{n_i}$ amounts to specifying its dependence structure or *copula*.

For example, if the $U_{i,s}$ ’s are mutually independent and $\text{pa}_i = s'$ was observed for some s' , then the abduction step will infer the distribution of $U_{i,s'}$ conditional on the observed data. This will tell us nothing about the $U_{i,s}$ ’s for $s \neq s'$, however. Alternatively, if $U_{i,1} = U_{i,2} = \dots = U_{i,n_i}$ then this models perfect positive dependency and inferring the conditional distribution of $U_{i,s'}$ in the abduction step amounts to simultaneously inferring the conditional distribution of all the $U_{i,s}$ ’s.

These considerations lead to a definition of the structural causal model where we explicitly account for this mechanism.

Definition 1. A *structural causal model (SCM)* over endogenous random variables $\mathbf{V} = (V_1, \dots, V_m)$ is given by a DAG \mathcal{G} over nodes \mathbf{V} , exogenous random vectors $\mathbf{U} = (\mathbf{U}_1^{n_1}, \dots, \mathbf{U}_m^{n_m})$ and functions f_1, \dots, f_m such that $V_i = f_i(\text{pa}_i, \mathbf{U}_i^{n_i})$ where $\text{pa}_i \subset \mathbf{V}$ are the parents of V_i in \mathcal{G} . Each $\mathbf{U}_i^{n_i}$ is an $n_i \times 1$ vector of $U(0, 1)$ random variables with joint distribution C_i . Finally each f_i can be represented as in (1).

Remark 1. Because of our ultimate focus on dynamic latent space models (see §4) we will continue to invoke Assumption 1 throughout the paper. In the context of Definition 1, this means we can assume that the $\mathbf{U}_i^{n_i}$ ’s in our SCM are independent, i.e. $\mathbf{U}_i^{n_i}$ is independent of $\mathbf{U}_j^{n_j}$ for $i \neq j$.

Figure 1b displays the SCM for our surgical procedure example. The only difference between the SCM in Figure 1a and Figure 1b is that in the latter figure we use $\mathbf{U}_O^{n_O}$ rather than U_O to represent the exogenous noise associated with V_O . Since neither V_H nor V_S have parents we can continue to

use U_H and U_S to represent their exogenous noise variables. (To be consistent with Definition 1, we should use $\mathbf{U}_H^{n_H}$ and $\mathbf{U}_S^{n_S}$ but since $n_H = n_S = 1$ we lose nothing in sticking with U_H and U_S .)

We emphasize that for causal questions related to association and intervention there is no need to introduce $\mathbf{U}_i^{n_i}$'s and Definition 1. This is because only counterfactual queries require the abduction step. That said, in many applications it seems that a single $U(0, 1)$ random variable U_i is assumed for all counterfactual queries. This amounts to assuming $U_{i,1} = U_{i,2} = \dots = U_{i,n_i}$ which, as mentioned earlier, leads to extreme positive dependency among the counterfactuals. While we haven't seen an SCM defined explicitly via vectors of $U(0, 1)$ random variables as in Definition 1, it should come as no surprise to those who work with counterfactuals and so we make no claims here regarding originality. Indeed we wouldn't be surprised if other researchers had also represented an SCM via (1) and Definition 1. For example, rather than introducing $\mathbf{U}_i^{n_i}$'s as we do above, [2] introduce so-called *response function* variables. Ultimately these response-function variables achieve the same goal as our representation in (1) although the approach seems quite difficult to follow.

2.3 An Alternative Definition of the SCM

To simplify our notation we define $V_i^{(s)}$ to denote the random variable $V_i \mid (\text{pa}_i = s)$. While Definition 1 and the $\mathbf{U}_i^{n_i}$'s are useful from a conceptual point of view, it will be more convenient to work with an alternative definition of the SCM. This is because in discrete-state space models there will be infinitely many joint distributions of $\mathbf{U}_i^{n_i}$ that all lead to the same joint distribution of $\{V_i^{(s)}\}_{s=1}^{n_i}$. In other words, the joint distribution of $\{V_i^{(s)}\}_{s=1}^{n_i}$ does not uniquely identify the joint distribution of $\mathbf{U}_i^{n_i}$. This is a consequence of Sklar's Theorem from the theory of copulas and is discussed in further detail in Appendix A. We will therefore take a more direct approach by directly modeling the joint distribution of $\{V_i^{(s)}\}_{s=1}^{n_i}$. This leads to an alternative (though essentially equivalent) and more practically useful definition of an SCM.

Definition 2. A structural causal model (SCM) over endogenous random variables $\mathbf{V} = (V_1, \dots, V_m)$ is given by a DAG \mathcal{G} over nodes \mathbf{V} . Each endogenous node V_i is associated with an n_i -dimensional cumulative distribution function (CDF) $\boldsymbol{\Pi}^{(i)}$ which is the joint CDF of $\{V_i^{(s)}\}_{s=1}^{n_i}$ where n_i is the number of possible settings of pa_i , the parents of V_i in \mathcal{G} .

As with Definition 1, we haven't seen an SCM defined explicitly via the joint CDF's of the $\{V_i^{(s)}\}_{s=1}^{n_i}$. But again, we make no claims of originality here since a representation such as this would be obvious to many. Indeed Pearl and his colleagues [2, 16, 19, 22], for example, work implicitly with such a representation when computing bounds on CQI's although they typically have static models with binary variables in mind. (In our our cheating-at-the-casino application in §4, we will use this representation at all the emission nodes of the HMM and use it to bound the expected winnings of the casino due to cheating.)

Dropping the superscript i , we refer to $\boldsymbol{\Pi}$ as the *counterfactual joint CDF* of node V , i.e. the joint CDF of $\{V^{(s)}\}_{s=1}^n$, and we use $\boldsymbol{\pi}$ for the corresponding probability mass function (PMF). That is,

$$\begin{aligned}\boldsymbol{\Pi}_{1\dots n}(v_1, \dots, v_n) &= P(V^{(1)} \leq v_1, \dots, V^{(n)} \leq v_n) \\ \boldsymbol{\pi}_{1\dots n}(v_1, \dots, v_n) &= P(V^{(1)} = v_1, \dots, V^{(n)} = v_n).\end{aligned}$$

Note that we can only ever observe one of these random variables at a time.

Before proceeding we make two observations:

1. We always assume the univariate *marginal* distributions of $\boldsymbol{\Pi}$ are known. This is a consequence of knowing the data-generating mechanism. For example, in our surgical procedure application we could easily estimate $P(V_O = \text{Good} \mid V_H = 1, V_S = 2)$ given sufficient data from procedures performed by similar surgeons at similar hospitals and on similar patients. But in general we assume we don't know the *joint* distribution $\{V_O \mid ((V_H, V_S) = s)\}_{s=1}^6$. In our casino application of §4, this amounts to knowing each of the initial, transition and emission distributions in the HMM. They can all be estimated given sufficient data.
2. As noted previously, a key step in estimating a counterfactual is the abduction step. In our SCM setting, this step can be executed as follows. If we observe $\text{pa}(V) = s'$ and $V^{(s')} = h$

then it is a simple exercise in probability to update Π (or π). For example,

$$P(v_1, \dots, v_{s'-1}, v_{s'+1}, \dots, v_n) \mid V^{(s')} = h = \frac{\pi_{1\dots n}(v_1, \dots, v_{s'-1}, h, v_{s'+1}, \dots, v_n)}{\pi_{s'}(h)}$$

where $\pi_{s'}$ is the marginal PMF of $V_{s'}$ which is easily computed from π . More generally, we may only have a distribution for $\text{pa}(V)$ and / or V conditional on a sequence of observations. We can then use further conditioning arguments to compute π' (the distribution of $\{V^{(s)}\}_{s=1}^n$ conditional on the observations) in terms of π . We do this in our HMM application in §4.

While we don't know the counterfactual distribution in general, we may be able to use domain specific knowledge to specify it or constrain it in some way. This is the subject of §3.

3 Modeling the Counterfactual Joint Distribution of V

We begin in §3.1 by identifying some important dependence structures or copulas that form interesting base cases. Then in §3.2 we discuss how bounds on counterfactual quantities might be computed. When properties like counterfactual stability [18] are imposed, then tighter bounds are obtained.

3.1 Specifying a Dependence Structure / Copula

Because the univariate marginal distributions of Π are known, we only need to specify the dependence structure or copula of Π . We consider three important base cases:

Independence. In this case $\Pi_{1\dots n}(v_1, \dots, v_n) = \Pi_1(v_1) \times \dots \times \Pi_n(v_n)$. We denote this joint distribution by Π^I and it models independence among the $V^{(s)}$'s.

Comonotonicity. In this case $\Pi_{1\dots n}(v_1, \dots, v_n) = \min\{\Pi_1(v_1), \dots, \Pi_n(v_n)\}$. We denote this joint distribution by Π^P and it represents the case of extreme positive dependence among the $V^{(s)}$'s.

Countermonotonicity. This only applies in the $n = 2$ -dimensional case and then $\Pi_{12}(v_1, v_2) = \max\{0, \Pi_1(v_1) + \Pi_2(v_2) - 1\}$. We denote this joint distribution by Π^N and it represents the case of extreme negative dependence among $V^{(1)}$ and $V^{(2)}$.

An explanation for these distributions as well as the interpretation we attached to them is in Appendix A. Note that all three base cases identify the joint distribution Π in terms of the known marginals.

Of course there are uncountably many copulas beyond these three copulas including, for example, parametric copulas such as the Gaussian, t and Archimedean copulas. Any of these copulas could be used to specify Π . It is also easily seen that convex combinations of copulas are copulas. For example we could take $\Pi = \lambda \Pi^I + (1 - \lambda) \Pi^P$ for some $\lambda \in [0, 1]$ and use this to represent a modeler's uncertainty regarding whether Π^I or Π^P is more appropriate in a given application.

Finally, we note that these copulas can be combined together to form copulas in higher dimensions. For example in an $n = 7$ -dimensional setting, it's possible that the copula of $(V^{(1)}, V^{(2)})$ is the countermonotonic copula, that of $(V^{(3)}, V^{(4)}, V^{(5)})$ is the independence copula and that of $(V^{(6)}, V^{(7)})$ is the comonotonic copula. Of course this doesn't uniquely specify the full 7-dimensional copula but it does highlight how domain specific knowledge might be used to reduce the space of feasible copulas and obtain tighter bounds for the counterfactual quantities of interest as we now discuss.

3.2 Computing Bounds

Let a denote the number of possible values of the node V . Then specifying the n -dimensional counterfactual joint CDF Π of V amounts to selecting a point on the a^n -dimensional simplex, i.e. the set of non-negative vectors in \mathbb{R}^{a^n} that sum to 1. In our setting the selection of such a point is constrained by knowing the univariate marginals. Other domain-specific information may also be available. For example, in the surgical procedure example, it may be reasonable to assume that the performances of the surgeons are mutually independent. Considerations such as this would help to constrain Π or equivalently (since the marginals are known) the copula.

If we can't uniquely identify the appropriate copula then we can formulate two optimization problems. The first problem maximizes the CQI while the second minimizes it. Both are optimization problems over the a^n -dimensional simplex. If the objective is linear (as will be the case in our cheating-casino application) then solving these bounds amounts to solving a linear program. If additional information or constraints on the copula are linear, then the feasible set for these optimization problems will be linear. For example, [18] propose *counterfactual stability* (CS) as being a desirable property for counterfactuals. Loosely speaking, the CS property can be stated as follows. Suppose we observe an outcome $V = v$ under some policy I . Then the counterfactual outcome of V under an interventional policy I' cannot be $V = v'$ (for $v' \neq v$) when $P'(V = v)/P(V = v) \geq P'(V = v')/P(V = v')$ where P and P' denote probabilities under the policies I and I' , respectively. In words, CS states that if $V = v$ was observed and this outcome becomes relatively more likely than $V = v'$ under the intervention, then the counterfactual value of V under the intervention cannot be v' . Whether or not imposing CS is appropriate will depend on the application but as we shall see in §4 we can easily impose it via linear constraints in our cheating-casino application. Moreover, it will follow immediately that there are infinitely many copulas in that application that satisfy CS and that picking one of them and generating counterfactuals from the resulting joint CDF is straightforward.

Time Consistency. In dynamic models where the state transitions etc. are homogeneous, i.e. time-independent, it is very natural to also assume that the copulas are time independent. We refer to this property as time consistency. For example, in the HMM of §4, we will need to work with a copula at each emission node of the graph. It seems reasonable to insist that this copula is time consistent. As we shall see, this results in much tighter bounds on the CQI.

Non-Linear Optimization Problems. While our cheating-casino application only requires the solution of LPs to compute lower and upper bounds on the CQI, in general these problems will be non-linear albeit over a linear constraint set. For example, if we want to compute the probability the patient would have survived if she had been permitted to take the regular scans, then bounding this probability will require the solution of non-linear and (one suspects) generally non-convex problems. These kinds of problems (where we optimize over a joint distribution subject to knowing the marginals) are sometimes called Fréchet problems and arise frequently, for example, in quantitative finance, e.g. [15]. For example, we may know the so-called value-at-risk of several individual portfolios but want to compute the worst-case value-at-risk when all of the portfolios are combined.

4 An Application: Cheating at the Casino

The framework developed above is general and we demonstrate its power via the *dishonest casino* [8, 12] application of a HMM. This application is well-known and often used to teach HMMs in machine learning courses [1, 7]. We discuss the HMM in §4.1, the CQI in §4.2, and results in §4.3.

4.1 A Dynamic Latent Space Model

The dishonest casino is a discrete-time HMM with T periods; see Figure 2. The hidden state $H_t \in \{1, 2\}$ for $t \in [T]$ denotes whether the casino is using a fair die ($H_t = 1$) or a loaded die ($H_t = 2$). Under a *fair* die, each of the six outcomes ($O_t \in \{1, \dots, 6\}$) is equally likely whereas under a *loaded* die, higher outcomes are more likely. The casino wins a reward of $w_i \in \mathbb{R}$ if the die rolls $i \in \{1, \dots, 6\}$ and w_i is increasing in i so the casino expects to win more under a loaded die.

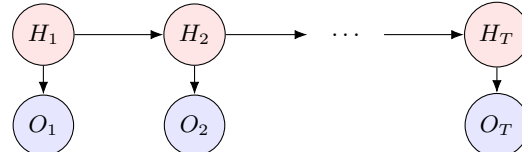


Figure 2: Dishonest casino. The states $H_{1:T}$ are hidden while the observations $O_{1:T}$ are observable.

We assume the data generating process, i.e. the initial state distribution $\mathbf{p} := [p_h]_{h \in \{1,2\}}$, the transition distribution matrix $\mathbf{Q} := [q_{hh'}]_{h,h' \in \{1,2\}}$, and the emission distribution matrix $\mathbf{E} := [e_{hi}]_{h \in \{1,2\}, i \in \{1, \dots, 6\}}$, are all known. More details on $(\mathbf{p}, \mathbf{Q}, \mathbf{E})$ are provided in Appendix B.1.

4.2 Expected Winnings Attributable to Cheating (EWAC)

We observed a path $o_{1:T}$ of die rolls which implies the casino won $w_{\text{obs}} := \sum_t w_{o_t}$. We now want to compute the expected winnings (of the casino) attributable to cheating or *EWAC*. Put another way, how much would the casino have won if they had been forced to use the fair die given the sequence of observed winnings? To answer this question we need the distribution of the *counterfactual path* $\tilde{O}_{1:T}$ where we use a “tilde” to denote counterfactuals. To do this we first condition on $o_{1:T}$, i.e. *abduction*, and then set $H_{1:T} = 1$, which is the *action* step. We then use $\tilde{O}_{1:T}$ to *predict* the counterfactual winnings $\sum_t w_{\tilde{O}_t}$, which is random since $\tilde{O}_{1:T}$ is so. Formally, we define

$$\text{EWAC} := w_{\text{obs}} - \sum_t \mathbb{E}[w_{\tilde{O}_t}]. \quad (2)$$

Our task here is *counterfactual off-policy evaluation* where the counterfactual policy is “no cheating ever” and the data comes from the policy of “occasional cheating according to the HMM”. Let $\pi(i, j) = \text{P}(O_t^{(1)} = i, O_t^{(2)} = j)$ be the joint counterfactual PMF where $O_t^{(h)} := O_t \mid (H_t = h)$. We invoked time consistency and so we have the same counterfactual joint distribution at each observation node. (Note that we don’t have to worry about the joint counterfactual distribution at the hidden-state nodes because the *action* step simply sets all of these nodes to 1.) We also define $g_t(h) := \text{P}(H_t = h \mid o_{1:T})$, which is easily computed via standard filtering and smoothing algorithms [3]. We now characterize EWAC in Proposition 1 and we prove it in Appendix B.2.

Proposition 1 (Characterization). *For any time-consistent π , EWAC satisfies*

$$\text{EWAC}(\pi) = w_{\text{obs}} - \sum_{t=1}^T \left\{ g_t(1) \times w_{o_t} + g_t(2) \times \sum_{i=1}^6 w_i \frac{\pi(i, o_t)}{e_{2,o_t}} \right\}. \quad (3)$$

Not surprisingly, EWAC depends on π which is the only unknown in our setup. As discussed in §3.1, one possibility here is to specify π via a copula such as the independence, comonotonic or countermonotonic copulas (see Appendix B.3) but the justification for doing this is likely to be lacking. Instead, we can simply obtain bounds on the EWAC. For an upper bound (UB), we maximize EWAC as in (3) with π as a matrix of decision variables. The feasible set \mathcal{F} ensures the joint PMF π satisfies the marginal constraints so that $\mathcal{F} = \{\pi \geq 0 : \sum_j \pi(i, j) = e_{1i} \forall i, \sum_i \pi(i, j) = e_{2j} \forall j\}$. Since (3) is linear in π , we obtain the following LP: $\text{EWAC}^{\text{ub}} := \max_{\pi \in \mathcal{F}} \text{EWAC}(\pi)$. A lower bound EWAC^{lb} is obtained by solving $\text{EWAC}^{\text{lb}} := \min_{\pi \in \mathcal{F}} \text{EWAC}(\pi)$. Note that π is constrained to be time-consistent as discussed in §3.2.

Counterfactual Stability (CS). Our framework allows us to be robust to the copula choice. We contrast this with [18], where one specifies a property of interest (CS) and implicitly derives via the Gumbel-max mechanism a generally non-unique SCM that satisfies it. In fact, as discussed in §3.2, our framework provides a systematic way to capture CS by simply adding CS constraints to the optimization. We can therefore characterize the *entire* space of SCMs that obey CS by modeling CS in our LP’s via the following linear constraints: $\pi(j, i) = 0$ for all $i \neq j$ such that $e_{1i}/e_{2i} \geq e_{1j}/e_{2j}$. (See Appendix B.4 for details.) Denoting by $\text{EWAC}_{\text{cs}}^{\text{ub}}$ and $\text{EWAC}_{\text{cs}}^{\text{lb}}$ the CS bounds, and by EWAC^* the EWAC under the true (unknown) copula, we obtain the following inequalities.

Proposition 2. $\text{EWAC}^{\text{lb}} \leq \text{EWAC}^* \leq \text{EWAC}^{\text{ub}}$ and $\text{EWAC}^{\text{lb}} \leq \text{EWAC}_{\text{cs}}^{\text{lb}} \leq \text{EWAC}_{\text{cs}}^{\text{ub}} \leq \text{EWAC}^{\text{ub}}$.

That is, EWAC^* always lies between EWAC^{lb} and EWAC^{ub} , and CS results in tighter bounds but the CS bounds may not be “legitimate” bounds on EWAC^* if the “true” copula does not satisfy CS.

4.3 Numerical Results

We parameterize (\mathbf{p}, \mathbf{Q}) via a scalar $\eta \in [0, 1]$, which quantifies the extent of cheating by the casino. Recall that EWAC is defined w.r.t. an observed path $o_{1:T}$ and as such, we analyze two paths, Path # 1 and Path # 2. On Path # 1 the sequence of observations happened to have an average of 3.5 which is what would be expected if a fair die had always been used. On Path # 2 the sequence of observations had an average of approx. 4.2. For each path, we consider all values of $\eta \in \{0.001, 0.002, \dots, 0.999\}$ with $\eta = 0$ and $\eta = 1$ denoting “always cheating” and “never cheating”, respectively. Further details are provided in Appendix B.5.

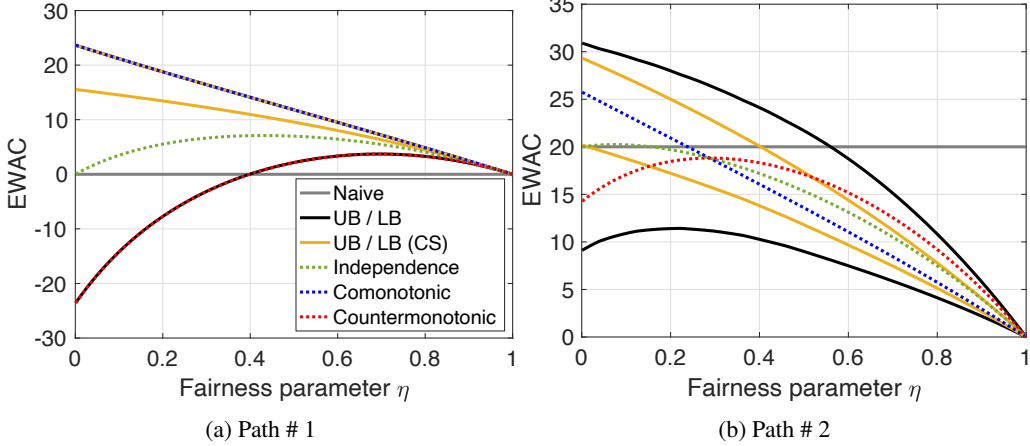


Figure 3: EWAC results. In Figure 3a, the UB, UB (CS), and comonotonic curves coincide (the highest curve in the figure), as do the LB and countermonotonic curves (the lowest curve).

Figure 3 displays the EWAC’s corresponding to seven different copulas - Π^I , Π^P and Π^N from §3.1, and the lower and upper bound copulas with and without CS constraints. In addition, we also plot a very naive estimate of EWAC which completely ignores the information in the observations, i.e. we fail to execute the abduction step. We note that imposing CS can result in a significant tightening of the bounds. For example, when $\eta = 0.2$ in Figure 3a, the (LB, UB) interval is approx. $[-10, 20]$ whereas the CS interval is much tighter at approx. $[12, 19]$. We also note that every point in the CS interval corresponds to a copula that satisfies the CS property. This resolves the open question of [18] regarding whether there are other causal mechanisms beyond the Gumbel-max mechanism that satisfy CS. In fact, our framework characterizes all SCMs consistent with CS.

As noted earlier, the counterfactual winnings are random because the *counterfactual path* $\tilde{O}_{1:T}$ is random. Given this randomness, we focused on the *expected* WAC but it is possible to understand the *distribution* of WAC by sampling $\tilde{O}_{1:T}$ via standard HMM sampling algorithms such as the FFBS algorithm, e.g. [3]. (Details and related results are provided in Appendix B.7.) This highlights the flexibility of our framework. The ability to simulate counterfactual paths is an important aspect of our framework and would be required in general to compute CQI’s in other applications. Finally, we imposed time-consistency on all the copulas in Figure 3; see also Proposition 1. Imposing time consistency is very natural and results in much tighter bounds. If we don’t impose time-consistency, then we obtain larger LPs that are nonetheless still very easy to solve. We explore this further in Appendix B.8. Finally, a considerably more detailed discussion of Figure 3 and some intuition for the patterns in the figure is provided in Appendix B.6.

5 Conclusions

We have provided a framework for conducting counterfactual off-policy evaluation that considers all possible causal mechanisms. We have shown by way of example that this framework allows us to compute lower and upper bounds on CQI’s in dynamic models with possibly latent states. To the best of our knowledge we are the first to do this. We also show how the CS property can be handled in our approach and how there are (infinitely) many causal mechanisms in general that are consistent with CS. When CS is justified, it can lead to much tighter bounds on the CQI.

There are many possible directions for future research. For example, it would be worthwhile considering other applications where bounds on the CQI can only be obtained by formulating and solving more challenging optimization problems than LPs. For another direction, recall from §3.2 that the size of the optimization problems grows exponentially in n , the number of settings of the parent nodes. These optimization problems might be challenging to solve in more complex models but it may still be possible to either solve or compute good bounds on their optimal solutions. Finally, it would also be interesting to consider other applications where domain specific knowledge allows us to impose tight constraints on the copulas.

References

- [1] Aarti Singh. 10-601 (CMU), 2011. URL https://www.cs.cmu.edu/~aarti/Class/10601/slides/HMM_11_1_2011.pdf.
- [2] Alexander Balke and Judea Pearl. Counterfactual probabilities: Computational methods, bounds and applications. In Ramon Lopez de Mantaras and David Poole, editors, *Uncertainty Proceedings 1994*, pages 46–54. Morgan Kaufmann, San Francisco (CA), 1994.
- [3] David Barber. *Bayesian Reasoning and Machine Learning*. Cambridge University Press, 2012.
- [4] Dimitri P. Bertsekas. *Dynamic Programming and Optimal Control: 1*. Athena Scientific, 2017.
- [5] Lars Buesing, Theophane Weber, Yori Zwols, Nicolas Heess, Sebastien Racaniere, Arthur Guez, and Jean-Baptiste Lespiau. Woulda, coulda, shoulda: Counterfactually-guided policy search. In *International Conference on Learning Representations*, 2019.
- [6] Zhihong Cai, Manabu Kuroki, Judea Pearl, and Jin Tian. Bounds on direct effects in the presence of confounded intermediate variables. *Biometrics*, 64(3):695–701, 2008.
- [7] Doug Downey. EECS 349 (Northwestern), 2010. URL https://users.cs.northwestern.edu/~ddowney/courses/349_Fall2010/lectures/hmmsML.pdf.
- [8] Richard Durbin, Sean R Eddy, Anders Krogh, and Graeme Mitchison. *Biological sequence analysis: Probabilistic models of proteins and nucleic acids*. Cambridge university press, 1998.
- [9] Peter Glynn and Søren Asmussen. *Stochastic Simulation: Algorithms and Analysis*. Springer, 2007.
- [10] Gurobi Optimization, LLC. Gurobi Optimizer Reference Manual, 2022. URL <https://www.gurobi.com>.
- [11] S. Kaufman, J.S. Kaufman, R.F. MacLenose, S. Greenland, and C. Poole. Improved estimation of controlled direct effects in the presence of unmeasured confounding of intermediate variables. *Statistics in Medicine*, 25:1683–1702, 2005.
- [12] Lin Himmelmann. Dishonest Casino, 2022. URL <https://search.r-project.org/CRAN/refmans/HMM/html/dishonestCasino.html>.
- [13] Guy Lorberbom, Daniel D. Johnson, Chris J Maddison, Daniel Tarlow, and Tamir Hazan. Learning generalized gumbel-max causal mechanisms. In M. Ranzato, A. Beygelzimer, Y. Dauphin, P.S. Liang, and J. Wortman Vaughan, editors, *Advances in Neural Information Processing Systems*, volume 34, pages 26792–26803. Curran Associates, Inc., 2021.
- [14] MATLAB. *Version 9.10.0 (R2021b)*. The MathWorks Inc., Natick, Massachusetts, 2021.
- [15] Alexander J. McNeil, Rüdiger Frey, and Paul Embrechts. *Quantitative Risk Management: Concepts, Techniques and Tools*. Princeton University Press, 2 edition, 2015.
- [16] Scott Mueller, Ang Li, and Judea Pearl. Causes of effects: Learning individual responses from population data. *arXiv*, 2021.
- [17] R.B. Nelsen. *An Introduction to Copulas*. Springer, 2 edition, 2006.
- [18] Michael Oberst and David Sontag. Counterfactual off-policy evaluation with Gumbel-max structural causal models. In Kamalika Chaudhuri and Ruslan Salakhutdinov, editors, *Proceedings of the 36th International Conference on Machine Learning*, volume 97 of *Proceedings of Machine Learning Research*, pages 4881–4890. PMLR, 09–15 Jun 2019.
- [19] Judea Pearl. *Causality*. Cambridge University Press, 2 edition, 2009.
- [20] Judea Pearl and Dana Mackenzie. *The Book of Why*. Penguin Books, 2018.
- [21] Abe Sklar. Fonctions de répartition à n dimensions et leurs marges. *Publ. Inst. Statist. Univ. Paris*, 8:229–231, 1959.

- [22] Jin Tian and Judea Pearl. Probabilities of causation: Bounds and identification. *Annals of Mathematics and Artificial Intelligence*, 8:287–313, 2000.
- [23] Stratis Tsirtsis, Abir De, and Manuel Rodriguez. Counterfactual explanations in sequential decision making under uncertainty. In M. Ranzato, A. Beygelzimer, Y. Dauphin, P.S. Liang, and J. Wortman Vaughan, editors, *Advances in Neural Information Processing Systems*, volume 34, pages 30127–30139. Curran Associates, Inc., 2021.

Appendices

A A Brief Introduction to Copulas

Copulas are functions that enable us to separate the marginal distributions from the dependency structure of a given multivariate distribution. They are particularly useful in applications where the marginal distributions are known (either from domain specific knowledge or because there is sufficient marginal data) but a joint distribution with these known marginals is required. This situation arises in many applications - for example in insurance and finance. In finance for example, the market prices of options on individual securities or indices can be used to compute the so-called risk-neutral (marginal) distributions for these securities. But if one is pricing an option on a basket of individual securities then the *joint* risk-neutral distribution is required. A similar situation arises with credit-default swaps (CDS). The market prices of CDS's can be used to infer the marginal risk-neutral probability of a company declaring bankruptcy by a certain date. But a collateralized debt obligation (CDO) depends on the *joint* risk-neutral distribution of the underlying companies going bankrupt. In our application in this paper, we know the marginal distribution of each random variable in $\{V_i^{(s)}\}_{s=1}^{n_i}$. (Recall that $V_i^{(s)} := V_i \mid (\text{pa}_i = s)$.) Indeed these marginal distributions can be estimated from data. But the *joint distribution* must be specified in order to compute counterfactuals.

In each of these cases one needs to work with a joint distribution with fixed or pre-specified marginal distributions. Copulas and Sklar's Theorem (see below) can be very helpful in these situations. We only briefly review some of the main results from the theory of copulas here but [17] can be consulted for an introduction to the topic. [15] also contains a nice introduction in the context of financial risk management.

Definition 3. A d -dimensional copula, $C : [0, 1]^d \rightarrow [0, 1]$ is a cumulative distribution function with uniform marginals.

We write $C(\mathbf{u}) = C(u_1, \dots, u_d)$ for a generic copula. It follows immediately from Definition 3 that $C(u_1, \dots, u_d)$ is non-decreasing in each argument and that $C(1, \dots, 1, u_i, 1, \dots, 1) = u_i$. It is also easy to confirm that $C(1, u_1, \dots, u_{d-1})$ is a $(d-1)$ -dimensional copula and, more generally, that all k -dimensional marginals with $2 \leq k \leq d$ are copulas. The most important result from the theory of copulas is Sklar's Theorem [21].

Theorem 1 (Sklar 1959). Consider a d -dimensional CDF Π with marginals Π_1, \dots, Π_d . Then there exists a copula C such that

$$\Pi(x_1, \dots, x_d) = C(\Pi_1(x_1), \dots, \Pi_d(x_d)) \quad (4)$$

for all $x_i \in [-\infty, \infty]$ and $i = 1, \dots, d$.

If Π_i is continuous for all $i = 1, \dots, d$, then C is unique; otherwise C is uniquely determined only on $\text{Ran}(\Pi_1) \times \dots \times \text{Ran}(\Pi_d)$ where $\text{Ran}(\Pi_i)$ denotes the range of the CDF Π_i .

Conversely, consider a copula C and univariate CDF's Π_1, \dots, Π_d . Then Π as defined in (4) is a multivariate CDF with marginals Π_1, \dots, Π_d .

A particularly important aspect of Sklar's Theorem in the context of this paper is that C is only uniquely determined on $\text{Ran}(\Pi_1) \times \dots \times \text{Ran}(\Pi_d)$. Because we are interested in applications with discrete state-spaces this implies that there will be many copulas that lead to the same joint distribution Π . It is for this reason that we prefer to work with our second definition of SCM (recall Definition 2), i.e. the definition that works directly with the joint distribution of $\{V_i^{(s)}\}_{s=1}^{n_i}$.

The following important result was derived independently by Fréchet and Hoeffding and provides lower and upper bounds on copulas.

Theorem 2 (The Fréchet-Hoeffding Bounds). Consider a copula $C(\mathbf{u}) = C(u_1, \dots, u_d)$. Then

$$\max \left\{ 1 - d + \sum_{i=1}^d u_i, 0 \right\} \leq C(\mathbf{u}) \leq \min\{u_1, \dots, u_d\}.$$

Three very important copulas are the comonotonic, countermonotonic (only when $d = 2$) and independence copulas which model extreme positive dependency, extreme negative dependency and (not surprisingly) independence. They are defined as follows.

Comonotonic Copula. The comonotonic copula is given by

$$C^P(\mathbf{u}) := \min\{u_1, \dots, u_d\} \quad (5)$$

which coincides with the Fréchet-Hoeffding upper bound. It corresponds to the case of extreme positive dependence. For example, let $\mathbf{U} = (U_1, \dots, U_d)$ with $U_1 = U_2 = \dots = U_d \sim U(0, 1)$. Then clearly $\min\{u_1, \dots, u_d\} = \Pi(u_1, \dots, u_d)$ but by Sklar's Theorem $F(u_1, \dots, u_d) = C(u_1, \dots, u_d)$ and so $C(u_1, \dots, u_d) = \min\{u_1, \dots, u_d\}$.

Countermonotonic Copula. The countermonotonic copula is a 2-dimensional copula given by

$$C^N(\mathbf{u}) := \max\{u_1 + u_2 - 1, 0\} \quad (6)$$

which coincides with the Fréchet-Hoeffding lower bound when $d = 2$. It corresponds to the case of extreme negative dependence. It is easy to check that (6) is the joint distribution of $(U, 1 - U)$ where $U \sim U(0, 1)$. (The Fréchet-Hoeffding lower bound is only tight when $d = 2$. This is analogous to the fact that while a pairwise correlation can lie anywhere in $[-1, 1]$, the *average* pairwise correlation of d random variables is bounded below by $-1/(d - 1)$.)

Independence Copula. The independence copula satisfies

$$C^I(\mathbf{u}) := \prod_{i=1}^d u_i$$

and it is easy to confirm using Sklar's Theorem that random variables are independent if and only if their copula is the independence copula.

A well known and important result regarding copulas is that they are invariant under monotonic transformations.

Proposition 3 (Invariance Under Monotonic Transformations). *Suppose the random variables X_1, \dots, X_d have continuous marginals and copula C_X . Let $T_i : \mathbb{R} \rightarrow \mathbb{R}$, for $i = 1, \dots, d$ be strictly increasing functions. Then the dependence structure of the random variables*

$$Y_1 := T_1(X_1), \dots, Y_d := T_d(X_d)$$

is also given by the copula C_X .

This leads immediately to the following result.

Proposition 4. *Let X_1, \dots, X_d be random variables with continuous marginals and suppose $X_i = T_i(X_1)$ for $i = 2, \dots, d$ where T_2, \dots, T_d are strictly increasing transformations. Then X_1, \dots, X_d have the comonotonic copula.*

Proof. Apply the *invariance under monotonic transformations* proposition and observe that the copula of (X_1, X_1, \dots, X_1) is the comonotonic copula. \square

B Further Details on the Dishonest Casino Application

B.1 HMM Primitives

A standard HMM (without the causal mechanism) has three primitives, namely the initial state distribution and the transition and emission matrices. We define them as follows for our dishonest casino application:

1. The **initial state distribution** is denoted by $\mathbf{p} := (p_1, p_2)$ where $p_h := \mathbb{P}(H_1 = h)$ for $h \in \{1, 2\}$.
2. The **transition matrix** is denoted by $\mathbf{Q} := [q_{hh'}]_{h,h' \in \{1,2\}}$ where $q_{hh'} := \mathbb{P}(H_{t+1} = h' | H_t = h)$ for $h, h' \in \{1, 2\}$ and $t \in [T - 1]$.
3. The **emission matrix** is denoted by $\mathbf{E} := [e_{hi}]_{h \in \{1,2\}, i \in \{1, \dots, 6\}}$ where $e_{hi} := \mathbb{P}(O_t = i | H_t = h)$ for $h \in \{1, 2\}$, $i \in \{1, \dots, 6\}$, and $t \in [T]$. If the hidden state is 1 (fair), then each outcome is equally likely, i.e., $e_{1i} = 1/6$ for all i .

The transition and emission matrices are time-independent although this is easily relaxed. We assume these matrices and initial distribution are known. (If this were not the case then it would be straightforward to estimate them, e.g. via the EM / Baum-Welch algorithm, [3], given sufficient observational data.)

B.2 Proof of Proposition 1

Proposition 1 (Characterization). *For any time-consistent π , EWAC satisfies*

$$\text{EWAC}(\pi) = w_{\text{obs}} - \sum_{t=1}^T \left\{ g_t(1) \times w_{o_t} + g_t(2) \times \sum_{i=1}^6 w_i \frac{\pi(i, o_t)}{e_{2, o_t}} \right\}. \quad (3)$$

Proof. We recall from (2) that

$$\text{EWAC} := w_{\text{obs}} - \sum_{t=1}^T \mathbb{E}[w_{\tilde{O}_t}]. \quad (2)$$

Note that our definition of the \tilde{O}_t 's from §4.2 entailed conditioning on the realized observation sequence $o_{1:T}$. Making this explicit, we obtain

$$\begin{aligned} \mathbb{E}[w_{\tilde{O}_t}] &= \mathbb{E}[w_{\tilde{O}_t} \mid o_{1:T}] \\ &= \underbrace{\mathbb{E}[w_{\tilde{O}_t} \mid o_{1:T}, H_t = 1] \mathbb{P}(H_t = 1 \mid o_{1:T})}_{=w_{o_t}} + \underbrace{\mathbb{E}[w_{\tilde{O}_t} \mid o_{1:T}, H_t = 2] \mathbb{P}(H_t = 2 \mid o_{1:T})}_{=g_t(2)} \quad (7) \end{aligned}$$

That $\mathbb{E}[w_{\tilde{O}_t} \mid o_{1:T}, H_t = 1] = w_{o_t}$ follows because $H_t = 1$ denotes the fair die was used at time t in which case $\tilde{O}_t = o_t$. Since $g_t(h) = \mathbb{P}(H_t = h \mid o_{1:T})$ is easily computed using standard filtering and smoothing algorithms [3], the only term in (7) that remains to compute is the term labelled (\star) .

Defining $O_t^{(h)} = O_t \mid (H_t = h)$, we obtain

$$\begin{aligned} (\star) := \mathbb{E}[w_{\tilde{O}_t} \mid o_{1:T}, H_t = 2] &= \mathbb{E}[w_{O_t^{(1)}} \mid O_t^{(2)} = o_t] \\ &= \sum_{i=1}^6 w_i \times \mathbb{P}(O_t^{(1)} = i \mid O_t^{(2)} = o_t) \\ &= \sum_{i=1}^6 w_i \times \frac{\mathbb{P}(O_t^{(1)} = i, O_t^{(2)} = o_t)}{\mathbb{P}(O_t^{(2)} = o_t)} \\ &= \sum_{i=1}^6 w_i \times \frac{\pi(i, o_t)}{e_{2, o_t}} \quad (8) \end{aligned}$$

where $\pi(i, j) = \mathbb{P}(O_t^{(1)} = i, O_t^{(2)} = j)$ is the counterfactual joint PMF as defined in §2.3. Putting (2), (7), and (8) together, we obtain (3). \square

B.3 Characterization of EWAC Under the Benchmark Copulas

We now provide a characterization of EWAC for each of the independence, comonotonic and countermonotonic copulas.

Proposition 5 (Characterization Under Copulas). *Let EWAC^I , EWAC^P and EWAC^N denote the EWAC for each of the independence, comonotonic and countermonotonic copulas, respectively. Then*

$$\begin{aligned} \text{EWAC}^I &= w_{\text{obs}} - \sum_{t=1}^T \left\{ g_t(1)w_{o_t} + g_t(2) \sum_{i=1}^6 w_i e_{1i} \right\} && \text{(independence)} \\ \text{EWAC}^P &= w_{\text{obs}} - \sum_{t=1}^T \left\{ g_t(1)w_{o_t} + g_t(2) \sum_{i=1}^6 w_i \frac{\pi^P(i, o_t)}{e_{2, o_t}} \right\} && \text{(comonotonic)} \\ \text{EWAC}^N &= w_{\text{obs}} - \sum_{t=1}^T \left\{ g_t(1)w_{o_t} + g_t(2) \sum_{i=1}^6 w_i \frac{\pi^N(i, o_t)}{e_{2, o_t}} \right\} && \text{(countermonotonic)} \end{aligned}$$

where for all (i, j)

$$\begin{aligned}\pi^P(i, j) &:= \sum_{\ell=0}^1 \sum_{\ell'=0}^1 (-1)^{\ell+\ell'} \min\{\boldsymbol{\Pi}_1(i-\ell), \boldsymbol{\Pi}_2(j-\ell')\} \\ \pi^N(i, j) &:= \sum_{\ell=0}^1 \sum_{\ell'=0}^1 (-1)^{\ell+\ell'} (\boldsymbol{\Pi}_1(i-\ell) + \boldsymbol{\Pi}_2(j-\ell') - 1)^+, \end{aligned}$$

and for $h \in \{1, 2\}$, $\boldsymbol{\Pi}_h(\cdot)$ is the CDF of $O_t^{(h)}$, i.e., $\boldsymbol{\Pi}_h(i) = P(O_t \leq i \mid H_t = h) = \sum_{j \leq i} e_{hj}$ for all i .

Proof. It follows from (3) that we simply need to characterize $\pi(i, o_t)$ under each of the three copulas. For the independence copula, we have

$$\begin{aligned}\pi^I(i, j) &= P(O_t^{(1)} = i, O_t^{(2)} = j) = P(O_t^{(1)} = i) \times P(O_t^{(2)} = j) \\ &= e_{1i} \times e_{2j} \end{aligned}$$

and we obtain EWAC^I. For the comonotonic and countermonotonic copulas, the following general fact proves useful:

$$\begin{aligned}\pi(i, j) &= P(O_t^{(1)} = i, O_t^{(2)} = j) \\ &= P(O_t^{(1)} \leq i, O_t^{(2)} \leq j) - P(O_t^{(1)} < i, O_t^{(2)} \leq j) \\ &\quad - P(O_t^{(1)} \leq i, O_t^{(2)} < j) + P(O_t^{(1)} < i, O_t^{(2)} < j) \\ &= \boldsymbol{\Pi}(i, j) - \boldsymbol{\Pi}(i-1, j) - \boldsymbol{\Pi}(i, j-1) + \boldsymbol{\Pi}(i-1, j-1) \\ &= \sum_{\ell=0}^1 \sum_{\ell'=0}^1 (-1)^{\ell+\ell'} \boldsymbol{\Pi}(i-\ell, j-\ell') \end{aligned} \tag{9}$$

where $\boldsymbol{\Pi}(i, j) = P(O_t^{(1)} \leq i, O_t^{(2)} \leq j)$ is the joint counterfactual CDF. Recalling that $\boldsymbol{\Pi}_h(i) = P(O_t^{(h)} \leq i)$ for all (h, i) , the comonotonic joint CDF $\boldsymbol{\Pi}^P$ satisfies

$$\begin{aligned}\boldsymbol{\Pi}^P(i, j) &= P(O_t^{(1)} \leq i, O_t^{(2)} \leq j) \\ &= P(\boldsymbol{\Pi}_1^{-1}(U) \leq i, \boldsymbol{\Pi}_2^{-1}(U) \leq j) \end{aligned} \tag{10a}$$

$$\begin{aligned}&= P(U \leq \boldsymbol{\Pi}_1(i), U \leq \boldsymbol{\Pi}_2(j)) \\ &= P(U \leq \min\{\boldsymbol{\Pi}_1(i), \boldsymbol{\Pi}_2(j)\}) \\ &= \min\{\boldsymbol{\Pi}_1(i), \boldsymbol{\Pi}_2(j)\} \end{aligned} \tag{10b}$$

where comonotonicity is invoked in (10a) with $U \sim \text{Uniform}(0, 1)$. Substituting (10b) into (9) yields

$$\pi^P(i, j) = \sum_{\ell=0}^1 \sum_{\ell'=0}^1 (-1)^{\ell+\ell'} \min\{\boldsymbol{\Pi}_1(i-\ell), \boldsymbol{\Pi}_2(j-\ell')\} \tag{11}$$

for all (i, j) . Finally, the countermonotonic joint counterfactual CDF satisfies

$$\begin{aligned}\boldsymbol{\Pi}^N(i, j) &= P(O_t^{(1)} \leq i, O_t^{(2)} \leq j) \\ &= P(\boldsymbol{\Pi}_1^{-1}(U) \leq i, \boldsymbol{\Pi}_2^{-1}(1-U) \leq j) \end{aligned} \tag{12a}$$

$$\begin{aligned}&= P(U \leq \boldsymbol{\Pi}_1(i), 1-U \leq \boldsymbol{\Pi}_2(j)) \\ &= P(U \leq \boldsymbol{\Pi}_1(i), U \geq 1-\boldsymbol{\Pi}_2(j)) \\ &= P(U \in [1-\boldsymbol{\Pi}_2(j), \boldsymbol{\Pi}_1(i)]) \end{aligned} \tag{12b}$$

$$= (\boldsymbol{\Pi}_1(i) + \boldsymbol{\Pi}_2(j) - 1)^+, \tag{12c}$$

where countermonotonicity is invoked in (12a) with $U \sim \text{Uniform}(0, 1)$, and $(\cdot)^+ := \max\{\cdot, 0\}$. Substituting (12b) into (9) yields

$$\pi^N(i, j) = \sum_{\ell=0}^1 \sum_{\ell'=0}^1 (-1)^{\ell+\ell'} (\boldsymbol{\Pi}_1(i-\ell) + \boldsymbol{\Pi}_2(j-\ell') - 1)^+ \tag{13}$$

for all (i, j) . \square

B.4 Modeling Counterfactual Stability via Linear Constraints

In the context of the dishonest casino HMM, counterfactual stability (CS) [18] can be expressed as follows. Recall that $e_{hi} = \text{P}(O^{(h)} = i)$ denotes the probability that observation equals i given the hidden state equals h . Now suppose that for arbitrary observations (i, j) such that $i \neq j$, we have

$$\frac{e_{1i}}{e_{21}} \geq \frac{e_{1j}}{e_{2j}}.$$

Then CS requires $\text{P}(O^{(1)} = j \mid O^{(2)} = i) = 0$ where we recall that $O_t^{(h)} = O_t \mid (H_t = h)$. That is, if i was observed and this outcome becomes relatively more likely than j under the intervention, then the counterfactual observation under the intervention cannot be j . (Recall that $H_t = 1$ and $H_t = 2$ denote the events that the fair and loaded die were used, respectively, at time t , and the intervention in question is that the casino employs a policy of always using the fair die.) Since

$$\text{P}(O^{(1)} = j \mid O^{(2)} = i) = \frac{\text{P}(O^{(1)} = j, O^{(2)} = i)}{\text{P}(O^{(2)} = i)} = \frac{\pi(j, i)}{e_{2j}},$$

we can model the CS property via following linear constraints:

$$\pi(j, i) = 0 \text{ for all } (i, j) \text{ such that } i \neq j \text{ and } \frac{e_{1i}}{e_{21}} \geq \frac{e_{1j}}{e_{2j}}. \quad (14)$$

B.5 Setup of the Numerical Experiments

In our numerical experiments of §4, we assume $T = 30$ periods and introduce a parameter $\eta \in [0, 1]$, which quantifies the degree of fairness in the HMM policy adopted by the casino. In particular, the initial state and transition distributions are given by

$$\mathbf{p} = (\eta, 1 - \eta)$$

$$\mathbf{Q} = \begin{bmatrix} \eta & 1 - \eta \\ \eta & 1 - \eta \end{bmatrix}.$$

That is, the initial state, i.e. die, is fair w.p. η and the next state is the same as the current state w.p. η as well. The emission distributions under the fair and loaded die obey

$$[e_{1i}]_i \propto (1, \dots, 1)$$

$$[e_{2i}]_i \propto (1, \dots, 6).$$

Finally, we set the casino's winnings to be $w_i := i$ for all i . Under this setup, the CS constraints (14) are simply $\pi(i, j) = 0$ for all $i > j$, i.e., $\text{P}(O_t^{(1)} > O_t^{(2)}) = 0$ for all t .

Recall that EWAC is defined w.r.t. an observed path $o_{1:T}$. The two paths we considered in §4.3 were defined as follows. Path # 1 equals

$$(1, 2, 3, 4, 5, 6, \dots, 1, 2, 3, 4, 5, 6),$$

with an average of 3.5. Path # 2 equals

$$(1, 2, 2, 3, 3, 3, 4, 4, 4, 4, 5, 5, 5, 5, 5, 6, 6, 6, 6, 6, 6, 1, 2, 3, 4, 4, 5, 5, 5, 5),$$

with an average of approximately 4.2. The first path therefore represents an unlucky path from the perspective of the casino adopted the cheating policy and yet only received a total payout that would have been average for a policy where it always used the fair die. The second path is more consistent with what might be expected under the cheating policy. For each path, we experiment with $\eta \in \{0.001, 0.002, \dots, 0.999\}$ so lower values of η correspond to casino using the loaded die (and therefore cheating) more frequently.

We coded in MATLAB [14] and used gurobi [10] to solve the LPs. Our computations took a total of less than 10 minutes on a 3.8 GHz 8-Core Intel Core i7 processor with 16 GB 2667 MHz DDR4 memory.

B.6 Further Discussion of the Numerical Results

In this appendix, we provide additional discussion of the EWAC results from §4.3. Recall that the naive estimate of EWAC does not condition on the observed sequence of die rolls and therefore completely ignores the abduction step. It simply calculates what the expected winnings would have been if the casino were to use a fair die on a fresh sequence of T die rolls and subtracts this from the observed winnings. To interpret naive EWAC, consider Path # 1 which corresponds to Figure 3a. Path # 1 is one where $w_{\text{obs}} = 105$ which happens to be the expected winnings under complete fairness (30×3.5). Accordingly, the naive estimate of EWAC is 0 on this path. In contrast, $w_{\text{obs}} = 125$ for Path # 2 and so the naive estimate of EWAC on this path is $125 - 105 = 20$. As we can see from Figure 3b (which corresponds to Path # 2), the naive estimate of EWAC can lie outside the interval $[\text{LB}, \text{UB}]$. This just serves to emphasize that there is no causal mechanism that is consistent with the naive estimate. Moreover, the naive estimate does not depend on η and is therefore constant in Figures 3a and 3b.

We now turn to EWAC^I , the EWAC under the independence copula. For Path # 1, we can see from Figure 3a that EWAC^I starts at 0 ($\eta = 0$) and ends at 0 ($\eta = 1$), with a peak in between. This behavior can be explained via the EWAC^I characterization from Proposition 5 in Appendix B.3. In particular, we have

$$\begin{aligned} \text{EWAC}^I &= w_{\text{obs}} - \sum_t \left\{ g_t(1)w_{o_t} + g_t(2) \sum_i w_i e_{1i} \right\} \\ &= w_{\text{obs}} - \sum_t \{g_t(1) \times o_t + g_t(2) \times 3.5\} \end{aligned} \quad (15)$$

since $e_{1i} = 1/6$ for all i and because we assumed $w_i = i$. When $\eta = 0$, the casino always uses the loaded die and hence $g_t(1) = 0$ and $g_t(2) = 1$ for all t . Since $w_{\text{obs}} = 105$ on this path we obtain $\text{EWAC}^I = 0$. Similarly, when $\eta = 1$, the casino always uses the fair die and hence $g_t(1) = 1$ and $g_t(2) = 0$ for all t . In this case, (15) again yields $\text{EWAC}^I = 0$ (since by definition $w_{\text{obs}} = \sum_t w_{o_t} = \sum_t o_t$). For intermediate values of η , periods t with a high value of o_t will typically have a higher value of $g_t(2)$ than periods with lower values of o_t . This is because the filtering / smoothing algorithm will generally infer that the loaded die is more likely to have been used when high die rolls, i.e. values of o_t , are observed. Referring to (15), this implies that more weight is placed on the 3.5 term than on the o_t term when o_t is high. Since the o_t 's have an average value of 3.5 and $\sum_t o_t = w_{\text{obs}}$, this explains the peaked behavior of EWAC^I in Figure 3a for intermediate values of η .

In the case of Path # 2 and Figure 3b, EWAC^I begins at 20 (when $\eta = 0$) and monotonically decreases to 0 at $\eta = 1$. This behavior can again be explained via (15). For example, when $\eta = 0$, $g_t(1) = 0$ and $g_t(2) = 1$ for all t and this implies $\text{EWAC}^I = w_{\text{obs}} - \sum_t 3.5 = 125 - 30 \times 3.5 = 20$. When $\eta = 1$, $g_t(1) = 1$ and $g_t(2) = 0$ for all t and this implies $\text{EWAC}^I = w_{\text{obs}} - \sum_t w_{o_t} = w_{\text{obs}} - w_{\text{obs}} = 0$.

The observation that all EWACs converge to 0 as $\eta \rightarrow 1$ can be explained via the general EWAC expression from Proposition 1:

$$\text{EWAC}(\boldsymbol{\pi}) = w_{\text{obs}} - \sum_t \left\{ g_t(1) \times w_{o_t} + g_t(2) \times \sum_i w_i \frac{\boldsymbol{\pi}(i, o_t)}{e_{2, o_t}} \right\}.$$

When $\eta = 1$ (casino never uses the loaded die), we have $g_t(1) = 1$ and $g_t(2) = 0$ for all t . Hence $\text{EWAC}(\boldsymbol{\pi}) = w_{\text{obs}} - \sum_t w_{o_t} = w_{\text{obs}} - w_{\text{obs}} = 0$ regardless of the causal mechanism / counterfactual joint distribution $\boldsymbol{\pi}$.

We also observe that an EWAC can be negative. In Figure 3a, for example, the countermonotonic EWAC, i.e. EWAC^N , is negative for small values of η . We can explain this using the EWAC^N characterization in Proposition 5 but instead we will provide an intuitive explanation. As discussed earlier, when $\eta = 0$, we have $g_t(1) = 0$ and $g_t(2) = 1$ for all t . This reflects the posterior certainty that the casino used a loaded die in every period. This in turn implies the casino should have made significantly more than 105 in expectation. However, Path # 1 corresponds to $w_{\text{obs}} = 105$, which implies the casino experienced a streak of “bad luck” despite always using the loaded die. The countermonotonic copula flips the “bad luck” into “good luck” (compare the U and $1 - U$ in (12a)),

and results in counterfactual winnings of over 105. Subtracting these counterfactual winnings from $w_{\text{obs}} = 105$, we obtain a negative EWAC^N . The same logic applies to non-zero but low values of η with Path # 1. Of course, if the countermonotonic curve is below 0, the LB has to be below 0 since by definition, LB is a lower bound (for *all* feasible copulas), and we clearly see this behavior for Path # 1 in Figure 3a.

In all of our results, we observe that EWAC^I lies between EWAC^P and EWAC^N . Under Path # 1, EWAC^P coincides with the UB copula and EWAC^N coincides with the LB copula. As demonstrated by Path # 2 and Figure 3b, this is not true in general, however, but they may serve as good approximations to the $[\text{LB}, \text{UB}]$ range. Furthermore, we observe that EWAC^P obeys the CS property under both paths (since it always lies between the corresponding bounds) but EWAC^I and EWAC^N can violate the CS property, e.g., Path # 1. Finally, we observe that even for a given path, the ordering among EWAC^I , EWAC^P and EWAC^N can vary with η . This is clear from Figure 3b.

B.7 Distribution of Winnings Attributable to Cheating (WAC)

The results in §4.3 focused on the *expected* WAC but it's also possible to estimate the *distribution* of WAC. Towards this end, consider an arbitrary counterfactual joint PMF π . This could be π^I , π^P or π^N , or the PMF corresponding to any of the four bounds. Our goal is to understand the distribution of WAC under the given π (conditional of course on the observed path $o_{1:T}$). To do so, we first generate B posterior samples of the hidden path via the FFBS algorithm [3]: $[h_{1:T}(b)]_{b=1}^B$. “Posterior” here corresponds to conditioning on $o_{1:T}$. Second, for each sampled path $b \in [B]$, we loop over each hidden state $h_t(b)$ for $t \in [T]$. If the hidden state equals fair ($h_t(b) = 1$), then the counterfactual observation equals the one we observed, i.e. $\tilde{O}_t(b) = o_t$. Otherwise $h_t(b) = 2$ and we use the joint distribution π conditioned on the observation o_t to sample $\tilde{O}_t(b)$. We therefore capture both sources of uncertainty, namely (1) the hidden state uncertainty via the FFBS algorithm and (2) the uncertainty in the counterfactual observation. Note that the first source of uncertainty does *not* depend on the causal mechanism, i.e. π , but the second step does.

In Figure 4 we display histograms of the WAC for four pairs of π for a value of $\eta = 0.5$ and for same two paths that were considered earlier. To map Figure 4 to Figure 3, note the average corresponding to each histogram in Figure 4 should match the value reported in Figure 3 (for $\eta = 0.5$). For example, in Figure 4a, the comonotonic histogram has an average around 12, which matches to the comonotonic value for $\eta = 0.5$ in Figure 3a. Under both the paths, the comonotonic histogram lies to the right of 0, and indeed we can easily show that $\text{WAC}^P \geq 0$ w.p. 1. We observe that the comonotonic and countermonotonic histograms are very similar to the UB and LB histograms, suggesting they might be able to serve as approximations to the bounds in other applications when the bounds are difficult to compute. (Of course one would need to provide some application-specific justification for making such an approximation.)

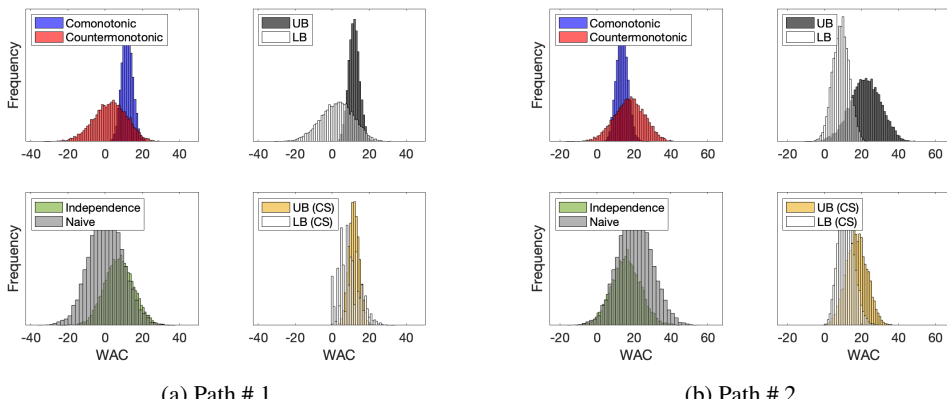


Figure 4: WAC distribution for $\eta = 0.5$.

B.8 Relaxing Time Consistency

As discussed in §3.2, it seems very reasonable to impose time consistency on the underlying joint PMF π , and we did so when computing bounds in our §4 numerics. Doing so shrinks the feasibility space of π in the underlying linear program (LP) and this leads to tighter bounds. To understand how much we gain (in terms of tightness of the bounds) by imposing time consistency, we now allow for time-varying copula / joint counterfactual distributions $[\pi^t]_t$ in the LP.

Recall the original lower bound LP from §4.2 was obtained by solving

$$\min_{\pi \in \mathcal{F}} \text{EWAC}(\pi),$$

where

$$\text{EWAC}(\pi) = w_{\text{obs}} - \sum_{t=1}^T \left\{ g_t(1) \times w_{o_t} + g_t(2) \times \sum_{i=1}^6 w_i \frac{\pi(i, o_t)}{e_{2, o_t}} \right\}$$

and $\mathcal{F} = \{\pi \geq 0 : \sum_j \pi(i, j) = e_{1i} \forall i, \sum_i \pi(i, j) = e_{2j} \forall j\}$.

We can relax the time-consistency constraint by simply allowing π to be time-varying. This leads to the following LP:

$$\min_{\pi^{1:T}} w_{\text{obs}} - \sum_{t=1}^T \left\{ g_t(1) \times w_{o_t} + g_t(2) \times \sum_{i=1}^6 w_i \frac{\pi^t(i, o_t)}{e_{2, o_t}} \right\} \quad (16a)$$

$$\text{s.t. } \pi^t \in \mathcal{F} \forall t \in [T] \quad (16b)$$

We can then solve (16) and the corresponding maximization problem to obtain lower and upper bounds on EWAC when we don't impose time-consistency. We do so for the same numerical setup of §4.3 and the results (analogous to Figure 3) are shown in Figure 5, with “time-varying” denoting the bounds obtained when we relax time consistency. Clearly, there is a lot of value in imposing time-consistency. (We did not include the naive, independence, comonotonic, and countermonotonic curves to avoid cluttering the figures.)

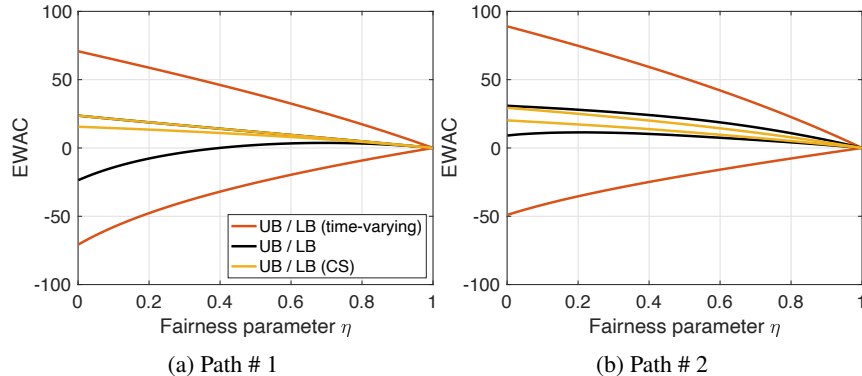


Figure 5: EWAC results with time-varying copula. In Figure 5a, the UB and UB (CS) curves coincide. The UB / LB and UB / LB (CS) curves are the same as in Figure 3.

We also note that the LP in (16) possesses a special structure which allows us to characterize its solution analytically. First, observe that it is separable w.r.t. t . We can then simplify the resulting period t objective (by omitting constants and scaling factors), and obtain the following LP for the period t PMF π^t :

$$\max_{\pi^t \in \mathcal{F}} \sum_{i=1}^6 w_i \pi^t(i, o_t). \quad (17)$$

(The minimization changes to a maximization due to the negative sign.) Not only is (17) lower dimensional than (16), its optimal solution exhibits the following closed-form:

$$\pi^t(i, o_t) = \min \left\{ e_{1i}, e_{2, o_t} - \sum_{k > i} \pi^t(k, o_t) \right\} \forall i. \quad (18)$$

To see why (18) holds, we suppose $o_t = 2$ for illustration and then consider the following 6-by-6 matrix of decision variables:

$\pi^t(1, 1)$	$\pi^t(1, 2)$	$\pi^t(1, 3)$	$\pi^t(1, 4)$	$\pi^t(1, 5)$	$\pi^t(1, 6)$	e_{11}
$\pi^t(2, 1)$	$\pi^t(2, 2)$	$\pi^t(2, 3)$	$\pi^t(2, 4)$	$\pi^t(2, 5)$	$\pi^t(2, 6)$	e_{12}
$\pi^t(3, 1)$	$\pi^t(3, 2)$	$\pi^t(3, 3)$	$\pi^t(3, 4)$	$\pi^t(3, 5)$	$\pi^t(3, 6)$	e_{13}
$\pi^t(4, 1)$	$\pi^t(4, 2)$	$\pi^t(4, 3)$	$\pi^t(4, 4)$	$\pi^t(4, 5)$	$\pi^t(4, 6)$	e_{14}
$\pi^t(5, 1)$	$\pi^t(5, 2)$	$\pi^t(5, 3)$	$\pi^t(5, 4)$	$\pi^t(5, 5)$	$\pi^t(5, 6)$	e_{15}
$\pi^t(6, 1)$	$\pi^t(6, 2)$	$\pi^t(6, 3)$	$\pi^t(6, 4)$	$\pi^t(6, 5)$	$\pi^t(6, 6)$	e_{16}

As dictated by \mathcal{F} , each row i needs to sum to e_{1i} and each column j to e_{2j} . Since (17) maximizes $\sum_i w_i \pi^t(i, 2)$ (recall $o_t = 2$), we focus on the second column which is highlighted in blue. Given that $w_1 < \dots < w_6$, it is optimal to set $\pi^t(6, 2)$ to be as big as possible and to move up greedily:

$$\begin{aligned}
\pi^t(6, 2) &= \min\{e_{16}, e_{22}\} \\
\pi^t(5, 2) &= \min\{e_{15}, e_{22} - \pi^t(6, 2)\} \\
\pi^t(4, 2) &= \min\{e_{14}, e_{22} - \pi^t(6, 2) - \pi^t(5, 2)\} \\
&\vdots \\
\pi^t(1, 2) &= \min\left\{e_{11}, e_{22} - \sum_{i>1} \pi^t(i, 2)\right\}.
\end{aligned}$$

Our expression in (18) simply generalizes this pattern. Note that the π^t variables in other columns are “free” and can be set arbitrarily as long as the constraints in \mathcal{F} are satisfied (since they do not appear in the objective). One can characterize the upper bound solution similarly by proceeding in the reverse order, i.e., from row 1 to row 6.